J|A|C|S
ARTICLES

Published on Web 11/12/2009

Macrocycles with Switchable *exo*/*endo* Metal Binding Sites

Lei-lei Tian,[†] Chun Wang,[†] Sandipan Dawn,[†] Mark D. Smith,[†] Jeanette A. Krause,[‡] and Linda S. Shimizu*,[†]

Department of Chemistry and Biochemistry, University of South Carolina, Columbia, South Carolina 29208, and The Richard C. Elder X-ray Crystallography Facility, Department of Chemistry, University of Cincinnati, Cincinnati, Ohio 45221

Received July 31, 2009; E-mail: shimizul@mail.chem.sc.edu

Abstract: We report herein the synthesis and metal complexation properties of two macrocyclic hosts that contain two 2,2′-bipyridines and two urea groups. These hosts take advantage of the conformationally mobile 5,5′-positions of the bipyridines to give metal binding sites that are dynamic. By simple bond rotation, these hosts can exchange an interior (*endo*) situated metal binding site for an exterior (*exo*) binding site. We examine the solid-state structures of the two free hosts and two coordination complexes ([Cd(host **1**)(H_2O)(NO_3)$_2$] and [Ag_2(host **2**)](SO_3CF_3)$_2$) using X-ray crystallography. Analysis of these crystal structures suggests that the bipyridine groups within the hosts are able to rotate to access multiple conformations including the desired *exo* and *endo* conformations. We also investigate the binding affinity of these new ligands in solution by UV−vis titrations with a series of metal nitrate salts (Ag, Cd, Zn, Ni, Mn, Fe, Co, Cr, and Cu) to afford discrete metal complexes. Some complexes showed a slow subsequent assembly to yield coordination polymers. Thus, these systems may afford unique insights into the process of metal organic framework formation.

Introduction

The synthesis and properties of macrocyclic compounds have been a priority in host−guest chemistry and molecular recognition because of their applications in ion transport,[1−5] chemosensing and imaging,[6−12] metallo-enzyme mimics,[13,14] catalysis, and nuclear waste treatment.[15] Cavity size and conformational flexibility are two important factors that determine the selectivity of macrocyclic hosts and their host−guest complex stability.[16−18] During the binding process the host undergoes conformational readjustment in order to arrange its binding sites complementary to the guest.[19] Although difficult to measure, rigidly preorganized hosts may have higher complexation activation energies that could lead to slower guest binding kinetics.[20−23] In contrast, conformationally mobile hosts may adjust rapidly to changing conditions and could be potentially more useful receptors in sensing applications because of their fast response time, reversible binding, and the possibility of detecting binding by means of altered conformations.[24−26] The interplay between rigidity and flexibility is a fascinating issue in supramolecular chemistry and is an area that we are beginning to explore with hosts that potentially contain dynamic *exo*/*endo* binding sites.

Our group has reported bis-urea macrocycles that are readily synthesized and self-assembled into columnar structures with guest accessible channels.[27−29] Our previous research has concentrated on adjusting the size and shape of the rigid macrocycles using different building blocks such as *m*-xylene, phenyl ether, or benzophenone. In this paper, we explored the

[†] University of South Carolina.
[‡] University of Cincinnati.

(1) Seo, J.; Park, S.; Lee, S. S.; Fainerman-Melnikova, M.; Lindoy, L. F. *Inorg. Chem.* **2009**, *48*, 2770–2779.
(2) Cazacu, A.; Tong, C.; Lee, A. V.; Fyles, T. M.; Barboiu, M. *J. Am. Chem. Soc.* **2006**, *128*, 9541–9548.
(3) Shamsipur, M.; Hashemi, O. R.; Lippolis, V. *J. Membr. Sci.* **2006**, *282*, 322–327.
(4) Barboiu, M.; Cerneaux, S.; van der Lee, A.; Vaughan, G. *J. Am. Chem. Soc.* **2004**, *126*, 3545–3550.
(5) Sidorov, V.; Kotch, F. W.; Kuebler, J. L.; Lam, Y. F.; Davis, J. T. *J. Am. Chem. Soc.* **2003**, *125*, 2840–2841.
(6) Kim, J. S.; Quang, D. T. *Chem. Rev.* **2007**, *107*, 3780–3799.
(7) Lindoy, L. F. *Dalton Trans.* **2006**, *43*, 5115–5117.
(8) Choi, K. H.; Hamilton, A. D. *J. Am. Chem. Soc.* **2003**, *125*, 10241–10249.
(9) Gawley, R. E.; Pinet, S.; Cardona, C. M.; Datta, P. K.; Ren, T.; Guida, W. C.; Nydick, J.; Leblanc, R. M. *J. Am. Chem. Soc.* **2002**, *124*, 13448–13453.
(10) Beer, P. D.; Gale, P. A. *Angew. Chem., Int. Ed.* **2001**, *40*, 486–516.
(11) Deetz, M. J.; Shang, M.; Smith, B. D. *J. Am. Chem. Soc.* **2000**, *122*, 6201–6207.
(12) Yang, X. G.; Knobler, C. B.; Zheng, Z. P.; Hawthorne, M. F. *J. Am. Chem. Soc.* **1994**, *116*, 7142–7159.
(13) Bakirci, H.; Koner, A. L.; Dickman, M. H.; Kortz, U.; Nau, W. M. *Angew. Chem., Int. Ed.* **2006**, *45*, 7400–7404.
(14) Izzet, G.; Douziech, E.; Prange, T.; Tomas, A.; Jabin, I.; Le Mest, Y.; Reinaud, O. *Proc. Natl. Acad. Sci. U.S.A.* **2005**, *102*, 6831–6836.
(15) Arnaud-Neu, F.; Schewing-Weill, M.-J.; Dozol, J.-F. Calixarene for Nuclear Waste Treatment. In *Calixarene 2001*; Asfari, Z., Böhmer, V., Harrowfield, J., Vicens, J., Eds.; Kluwer Academic Publishers: Dordrecht, 2001; pp 642−662.
(16) Kuhnert, N.; Burzlaff, N.; Patel, C.; Lopez-Periago, A. *Org. Biomol. Chem.* **2005**, *3*, 1911–1921.
(17) Takemura, H. *Curr. Org. Chem.* **2005**, *9*, 521–533.
(18) Kaplan, W. A.; Suslick, K. S.; Scott, R. A. *J. Am. Chem. Soc.* **1991**, *113*, 9824–9827.
(19) Filby, M. H.; Steed, J. W. *Coord. Chem. Rev.* **2006**, *250*, 3200–3218.
(20) Moore, J. S. *Angew. Chem., Int. Ed.* **2006**, *45*, 4416–4439.
(21) MacLachlan, M. J. *Pure Appl. Chem.* **2006**, *78*, 873–888.
(22) Hoger, S. *Angew. Chem., Int. Ed.* **2005**, *44*, 3806–3808.
(23) Moore, J. S. *Chem. Commun.* **2003**, 807–818.
(24) Hodacova, J.; Budesinsky, M. *Org. Lett.* **2007**, *9*, 5641–5643.
(25) Riddle, J. A.; Jiang, X.; Lee, D. W. *Analyst* **2008**, *133*, 417–422.
(26) Misra, R.; Chandrashekar, T. K. *Acc. Chem. Res.* **2008**, *41*, 265–279.

10.1021/ja906474z CCC: $40.75

feasibility of incorporating bipyridine functional groups in the macrocyclic framework through connections that tolerate bond rotation. The two macrocyclic hosts each contain two 2,2′-bipyridine units that can freely rotate. These bipyridines are bridged by either free ureas (host **1**) or triazinanone-protected ureas (host **2**). Simple bond rotation should enable the metal binding sites to flip from the interior of the macrocycle to its exterior and give rise to different conformational isomers. To test if this "switchable" design would affect the host's ability to bind metals, we examined a series of host metal complexes in both the solid state and in solution. We compared their structure and binding affinity with what has been observed for other bipyridines. Metal cations that match the interior of the hosts by having suitable ionic radii and coordination preferences for the geometrically constrained set of bipyridines were expected to show a preference for binding inside the cavity (*endo*). In contrast, metals with other coordination preferences or with larger ionic radii were expected to prefer to bind to the host when the bipyridines are rotated outward in an *exo* orientation. Therefore, the metal binding event should shift the host to the conformation most suitable for complexation.

Further assembly of these discrete metal−ligand complexes either by metal coordination of the macrocycles that adopt *exo* conformations or by hydrogen bonding of the ureas should yield coordination polymers or metal organic frameworks (MOFs). MOFs are a new class of porous materials that are able to absorb molecules ranging in size from H_2 to large buckyballs.[30−34] Currently, a number of groups are exploring methods to incorporate functionality into MOFs to modulate their physical and chemical properties.[35−40] Strategies include preinstallation of the functional groups prior to or during the synthesis of the MOFs or by "postsynthetic modification".[35−40] Indeed, recently urea functionalized MOFs have been synthesized through postsynthetic modification of Yaghi's isoreticular metal-organic framework-2 (IRMOF-3).[39,40] Sometimes the MOF fails to crystallize into the desired structure because of the presence of the new functional groups. In these cases, it is difficult to discern if the functional group has interrupted the metal−ligand interactions that are central to MOF formation or if other factors are to blame. The macrocycles reported in this manuscript have the potential to evaluate the metal−ligand assembly in the presence of the urea functional groups. They enable the study of the initial coordination events in solution and allow us to examine their further assembly by spectroscopic methods. Thus, these systems could provide unique insight into the process of MOF synthesis.

Linear ligands that contain two or more 2,2′-bipyridine units[41,42] have been used to connect metal centers in a well-defined spatial arrangement for applications in sensing,[43,44] helical assembly,[45] chiral molecular recognition,[46,47] photonics and optoelectronics, and electrochemistry applications.[48−50] The 2,2′-bipyridine group has also be incorporated into macrocycles, which may constrain the metal binding site to a well-defined size and shape. This special feature of macrocycles has the potential to enhance the ligand's selectivity toward particular metal ions of complementary size. For example, two 2,2′-bipyridines can be connected at positions 4 and 4′ to yield macrocycles that direct the coordination sites to the exterior of the macrocyclic cavity. These *exo*-ligands are used as building blocks for the construction of one-dimensional coordination polymers[51] or binuclear complexes with interesting electrochemical properties.[52] Alternatively, connection of the 2,2′-bipyridines at positions 6 and 6′ affords macrocycles with interior coordination sites. These *endo*-ligands have the two bipyridines preorganized for binding and are capable of complexation of specific metal cations with complementary size.[53,54] Few macrocycles have been reported that connect the 2,2′-bipyridines through their 5,5′ positions as this connection allows for both *exo* and *endo* coordination modes.[55−61] A phenylacetylene macrocycle from Schlüter's group with two opposing 2,2′-bipyridines can coordinate with 2 equiv of $[Ru(bipy)_2Cl_2]$ to form the doubly *exo*-cyclical complex (Figure 1c).[59] As a result of the large cavity size (∼13.7 Å × 7.3 Å)[60] and relatively rigid

(27) Yang, J.; Dewal, M. B.; Profeta, S.; Smith, M. D.; Li, Y.; Shimizu, L. S. *J. Am. Chem. Soc.* **2008**, *130*, 612–621.
(28) Dewal, M. B.; Xu, Y.; Yang, J.; Mohammed, F.; Smith, M. D.; Shimizu, L. S. *Chem. Commun.* **2008**, 3909–3911.
(29) Shimizu, L. S.; Hughes, A. D.; Smith, M. D.; Davis, M. J.; Zhang, B. P.; zur Loye, H.-C.; Shimizu, K. D. *J. Am. Chem. Soc.* **2003**, *125*, 14972–14973.
(30) Eddaoudi, M.; Moler, D. B.; Li, H.; Chen, B.; Reineke, T. M.; O'Keefe, M.; Yaghi, O. M. *Acc. Chem. Res.* **2001**, *34*, 319–330.
(31) Ockwig, M. W.; Delgado-Friedrich, O.; O'Keefe, M.; Yaghi, O. M. *Acc. Chem. Res.* **2005**, *38*, 176–182.
(32) Ferey, G.; Mellot-Draznieks, C.; Serre, C.; Millange, F. *Acc. Chem. Res.* **2005**, *38*, 217–225.
(33) Robson, R. *J. Chem. Soc., Dalton Trans.* **2000**, 3735–3744.
(34) Tranchemontagne, D. J.; Medoza-Cortes, J. L.; O'Keefe, M.; Yaghi, O. M. *Chem. Soc. Rev.* **2009**, *38*, 1257–1283.
(35) Seo, J. S.; Whang, D.; Lee, H.; Jun, S. I.; Oh, J.; Jeon, Y. J.; Kin, K. *Nature* **2000**, *404*, 982–986.
(36) Mulfort, K. L.; Hupp, J. T. *J. Am. Chem. Soc.* **2007**, *129*, 9604–9605.
(37) Costa, J. S.; Gamez, P.; Black, C. A.; Roubeau, O.; Teat, S. J.; Reedik, J. *Eur. J. Inorg. Chem.* **2008**, 1551–1554.
(38) Wang, Z. Q.; Cohen, S. M. *Angew. Chem., Int. Ed.* **2008**, *47*, 4699–4702.
(39) Wang, Z. Q.; Cohen, S. M. *J. Am. Chem. Soc.* **2007**, *129*, 12368–12369.
(40) Dugan, E.; Wang, Z.; Okamura, M.; Medina, A.; Cohen, S. M. *Chem. Commun.* **2008**, 3366–3368.
(41) Albrecht, M. *Chem. Rev.* **2001**, *101*, 3457–3497.
(42) Kaes, C.; Katz, A.; Hosseini, M. W. *Chem. Rev.* **2000**, *100*, 3553–3590.
(43) Torrado, A.; Imperiali, B. *J. Org. Chem.* **1996**, *61*, 8940–8948.
(44) Josceanu, A. M.; Moore, P.; Rawle, S. C.; Sheldon, P.; Smith, S. M. *Inorg. Chim. Acta* **1995**, *240*, 159–168.
(45) Piguet, C.; Bernardinelli, G.; Hopfgartner, G. *Chem. Rev.* **1997**, *97*, 2005–2062.
(46) Knof, U.; von Zelewsky, A. *Angew. Chem., Int. Ed.* **1999**, *38*, 302–322.
(47) Belser, P.; Bernhard, S.; Jandrasics, E.; von Zelewsky, A.; DeCola, L.; Balzani, V. *Coord. Chem. Rev.* **1997**, *159*, 1–8.
(48) Belser, P.; Bernhard, S.; Blum, C.; Beyeler, A.; De Cola, L.; Balzani, V. *Coord. Chem. Rev.* **1999**, *190−192*, 155–169.
(49) Balzani, V.; Juris, A.; Venturi, M.; Campagna, S.; Serroni, S. *Chem. Rev.* **1996**, *96*, 759–833.
(50) Baxter, S. M.; Jones, W. E.; Danielson, E.; Worl, L.; Strouse, G.; Younathan, J.; Meyer, T. J. *Coord. Chem. Rev.* **1991**, *111*, 47–71.
(51) Kaes, C.; Hosseini, M. W.; Rickard, C. E. F.; Skelton, B. W.; White, A. H. *Angew. Chem., Int. Ed.* **1998**, *37*, 920–922.
(52) Kaes, C.; Hosseini, M. W.; DeCian, A.; Fischer, J. *Tetrahedron Lett.* **1997**, *38*, 3901–3904.
(53) Ibrahim, R.; Tsuchiya, S.; Ogawa, S. *J. Am. Chem. Soc.* **2000**, *122*, 12174–12185.
(54) Tsuchiya, S.; Nakatani, Y.; Ibrahim, R.; Ogawa, S. *J. Am. Chem. Soc.* **2002**, *124*, 4936–4937.
(55) De Mendoza, J.; Mesa, E.; Rodriguez-Ubis, J. C.; Vázquez, P.; Vögtle, F.; Windscheif, P. M.; Rissanen, K.; Lehn, J. M.; Lilienbaum, D.; Ziessel, R. *Angew. Chem., Int. Ed.* **1991**, *30*, 1331–1333.
(56) Nitschke, J.; Tilley, T. D. *J. Org. Chem.* **1998**, *63*, 3673–3676.
(57) Nitschke, J.; Zürcher, S.; Tilley, T. D. *J. Am. Chem. Soc.* **2000**, *122*, 10345–10352.
(58) Nitschke, J.; Tilley, T. D. *Angew. Chem., Int. Ed.* **2001**, *40*, 2142–2145.
(59) Henze, O.; Lentz, D.; Schafer, A.; Franke, P.; Schluter, A. D. *Chem.—Eur. J.* **2002**, *8*, 357–365.
(60) The cavity size was calculated from the crystal structure provided by ref 59.
(61) Baxter, P. N. W. *J. Org. Chem.* **2001**, *66*, 4170–4179.

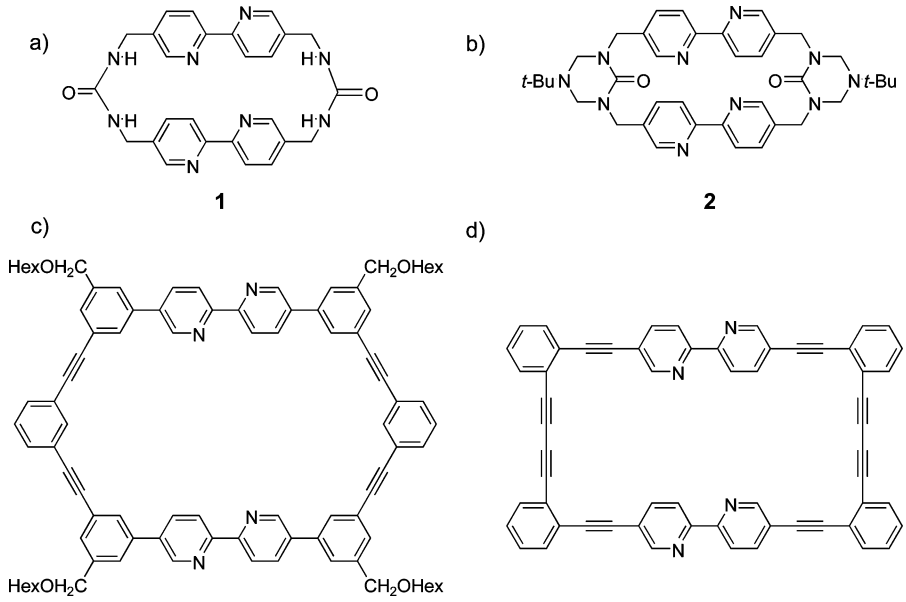

Figure 1. Comparison of bipyridine macrocycles that allow the binding sites to "flip" dynamically between *exo* and *endo* conformations. (a) Host **1** (~8.2 Å × 2.0 Å); (b) host **2** (~7.9 Å × 3.0 Å); (c) the phenylacetylene macrocycle (~13.7 Å × 7.3 Å);[59] (d) the twistophane macrocycle.[61]

Scheme 1. Schematic Representation of the Coordination Modes in Macrocycles That Are Able To Flip the Coordination Site from an Interior (*endo*) to an Exterior (*exo*) Position

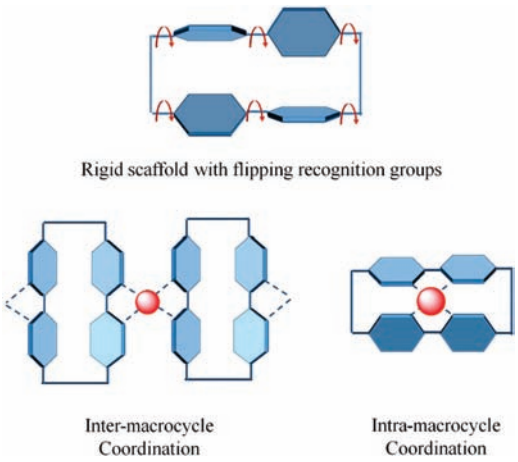

architecture, only *exo*-coordination was observed. Baxter reported a dehydroannulene framework that incorporated two 2,2′-bipyridine units into a chiral twisted architecture with a small central void (Figure 1d). The cavity enforced a tetrahedral arrangement of nitrogen lone pair electrons to favor *endo* coordination of metals and showed potential applications in the detection and monitoring of Zn^{2+} in biological media.[61]

In comparison, the metal binding sites in hosts **1** and **2** should dynamically flip between exterior and interior positions (Scheme 1). Thus both *exo* and *endo* coordination modes should be accessible, and the metal coordination preference, size, and shape should dictate which coordination conformation is favored. Given the relatively small cavity size of hosts **1** and **2** (~ 8.2 Å × 2.0 Å for **1** and ~ 7.9 Å × 3.0 Å for **2**), we predicted that *endo* coordination could be possible for smaller transition metal ions that preferred to form tetrahedral, square planar, or octahedral complexes. Hosts **1** and **2** were screened for their ability to bind a series of metal salts using UV−vis spectroscopy. Binding stoichiometries were evaluated by JOB plot analysis, and the association constants were estimated using a nonlinear least-squares regression method. The two macrocycles showed different host:guest stoichiometries when screened against a series of metal guests. Tetradentate host **1** prefers mononuclear complexes, whereas host **2** prefers to form binuclear complexes. This difference is likely due to the presence of additional basic tertiary aliphatic amines on the triazinanone groups, which makes this host a hexadentate ligand. In addition, the rigidity of the fused six-membered ring of the triazinanone as well as the sterics of the attached *tert*-butyl group also affects the structure of the coordination complexes. These different binding modes also play a role in the further supramolecular assembly of these small complexes, and we probed these assembled structures by X-ray crystallography and light scattering.

Results and Discussion

Our target macrocycles incorporated two 5,5′-disubstituted 2,2′-bipyridine and two ureas (free ureas **1** or triazinanone-protected ureas **2**) with flexible methylene connections. We used molecular modeling to probe the conformations of these macrocycles. A Monte Carlo search using Spartan[62] with MMFF predicted that in the lowest energy structures of the macrocycles **1** and **2** are quite similar, and the 2,2′-bipyridine units adopt *anti*-coplanar configurations with the pyridine nitrogens nearly perpendicular to the macrocycle plane (Figure 2). Such a conformation provides a central void, in which the distance between the van der Waals surfaces of diagonal pyridyl nitrogen atoms was estimated as 3.2−3.0 Å.[63] Parallel alignment of the 2,2′-bipyridine units with respect to the plane of the macrocycle forms the smallest recognition site (~1 Å). In solution, free rotation of 2,2′-bipyridine units provides an adjustable cavity that should be able to accommodate most transition metals, whose ionic radii typically range between 0.5−1.8 Å. Although the two macrocycles have many similarities, host **1** contains

(62) *Spartan 04 for Macintosh*, v 1.1.1; Wavefunction, Inc.: Irvine, CA., 2007.

(63) Distance between van der Waals surfaces of atoms was calculated as (internuclear distance)−(sum of van der Waals radii of atoms involved). The distance between the van der Waals surfaces of two opposite pyridyl nitrogen atoms.

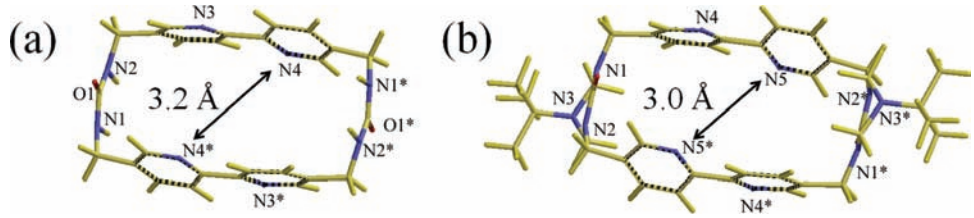

Figure 2. Spartan calculated models of the host **1** and host **2**.[62] Monte Carlo searches of the conformer distribution at ground state with Molecular Mechanics (MMFF) suggest the lowest energy structures of (a) host **1** and (b) host **2** do not adopt either *exo* or *endo* conformations. The distance between the van der Waals surfaces of the pore defining pyridine nitrogens is estimated as 3.2 and 3.0 Å, respectively.

Scheme 2. Synthesis of Bipyridine-Containing Hosts

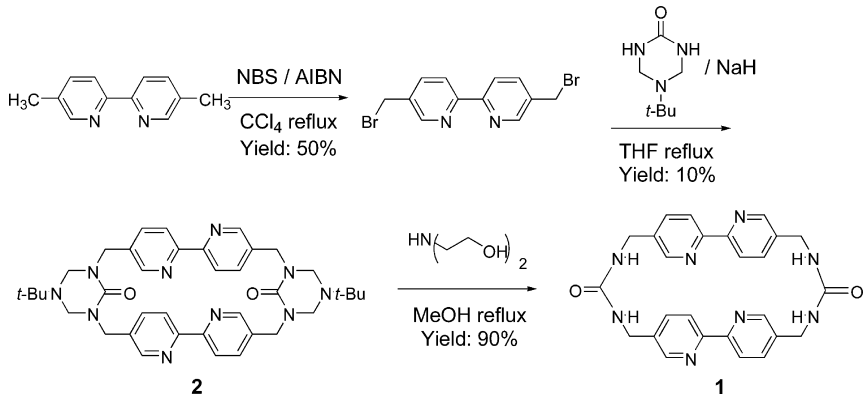

free urea units, which are superb hydrogen-bonding groups as well as potential sites for anion binding. In comparison, host **2** contains no hydrogen bond donors but has basic tertiary aliphatic nitrogens within the triazinanone group that could be a potential site for polynuclear coordination complexes.

The next step was to synthesize these hosts and to study their solid-state structures to see what conformations they adopt. Bis-urea macrocycle **2** was synthesized in two steps. Bromination of 5,5′-dimethyl-2,2′-dipyridyl with *N*-bromosuccinimide afforded the dibromide, which cyclized under basic conditions with triazinanone to yield the triazinanone-protected host **2** (Scheme 2). Colorless plate crystals of **2** suitable for X-ray diffraction studies were grown by slow diffusion of *n*-hexane into a saturated dichloromethane solution of host **2**. The triazinanone groups were deprotected to the ureas with diethanolamine in acidic water/methanol to afford host **1** (90% yield), which formed crystals suitable for X-ray diffraction upon cooling of the deprotection solution.

We next compared the solid-state structures of macrocycles **1** and **2**. The crystal structures provide a conformational "snapshot", and the macrocycles are likely to adopt different conformations in solution. The two hosts have similar structures in the solid state (Figure 3). Both are centrosymmetric, with the two urea carbonyls pointed in opposite directions. Neither host displayed the proposed *exo*- or *endo*-bipyridine conformations. Instead, much like Spartan predictions, the 2,2′-bipyridine units adopted twisted *anti* conformations with N3−C5−C8−N4 dihedral angles for **1** of 24.6° and N4−C7−C10−N5 for **2** of 32.1°. Two diagonal nitrogen atoms face inward toward the macrocycle ring (with dihedral angles of 67.2° for **1** and 60.2° for **2**) with the other two diagonal nitrogen atoms pointing outward the macrocycle (with dihedral angles of 38.6° for **1** and 40.1° for **2**). The void spaces of these cavities calculated from the crystal structures are smaller than the theoretical predictions from Spartan calculations in the gas phase.[63] The cavity size for coordination was determined by the distance

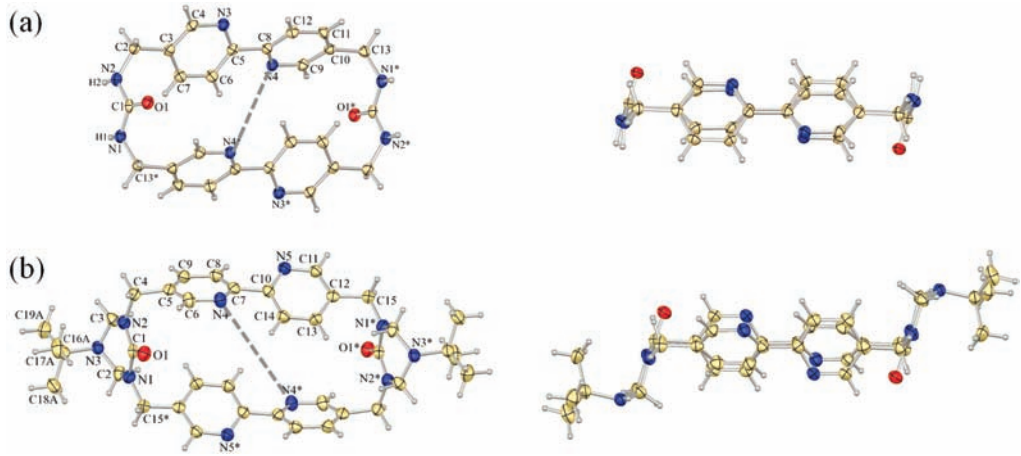

Figure 3. X-ray crystal structure of (a) macrocycle **1** and (b) macrocycle **2** with top view and side view, respectively. The distance between the van der Waals surfaces of two opposite pyridyl nitrogen atoms (N4 to N4a, dashed line) is about 2.0 Å for **1** and 3.0 Å for **2**.

Table 1. Ionic Radii of Some Commonly Used Metal Ions[a]

	Cr^{3+}	Mn^{2+}	Fe^{3+}	Co^{2+}	Ni^{2+}	Cu^{2+}	Zn^{2+}	Cd^{2+}	Ag^{+}
radius (Å)	0.62	0.83	0.65	0.75	0.69	0.73	0.74	0.95	1.00

[a] Values are for six-coordination, with the exception of Ag, which is for four-coordination.[64]

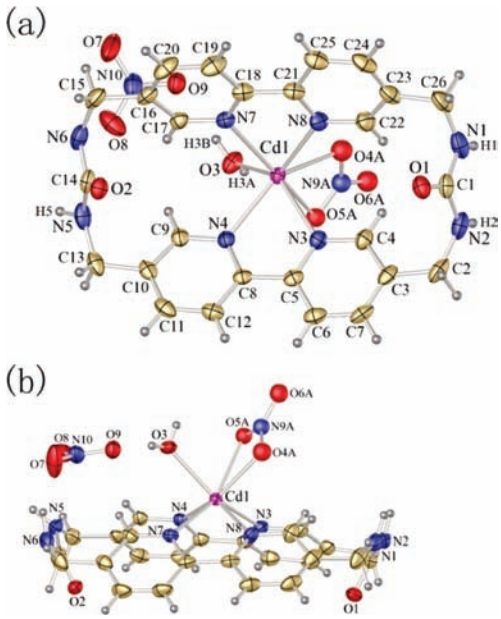

Figure 4. Crystal structure of complex [Cd(Ligand **1**)$(H_2O)(NO_3)_2$]. (a) Top view of displacement ellipsoid plot with ellipsoids drawn at the 40% probability level. The minor nitrate disorder component was omitted, and atom H6 was obscured. (b) Side view showing the tilting of H6 toward the nitrate O7.

between the van der Waals surfaces of two opposite pyridyl nitrogen atoms (N4 to N4a). The value is approximately 2.0 Å for **1** and 3.0 Å for **2**. In solution, we expect that the bipyridine rings freely rotate and access the *exo* and *endo* conformations that are preorganized for metal complexation. Given both Spartan calculations and X-ray data, we investigated metal cations with van der Waals radii of ≤1 Å (Table 1) as these should be free to form complexes with both the *endo* and *exo* conformations of the two hosts.

Crystal Structure of Host·Metal Complexes. We next investigated the formation of host·metal complexes. The hosts were individually mixed in 1:1 ratio with metal salts [$AgCF_3SO_3$, $AgNO_3$, $Cd(NO_3)_2$, $Zn(CF_3SO_3)_2$, $Zn(NO_3)_2$, $Cu(NO_3)_2$, and $Ni(NO_3)_2$]. We used slow evaporation methods for crystallization of the less soluble host **1** in THF (10^{-5}−10^{-4} mol L^{-1}). The greater solubility of host **2** allowed the use of solvent diffusion methods in which the metal salts were dissolved in MeOH and layered on top of a solution of **2** in CH_2Cl_2 (10^{-3}−10^{-2} mol L^{-1}). X-ray quality single crystals were obtained for the host **1**·Cd^{2+} and host **2**·Ag^{+} complexes. Colorless plates of **1**·Cd^{2+} were obtained by slow evaporation of the mixture of **1** and $Cd(NO_3)_2$ in THF (10^{-5} M, 1:1 molar ratio). The crystal structure revealed the formation of the mononuclear neutral complex Cd(**1**)$(H_2O)(NO_3)_2$ with a 1:1 host:guest stoichiometry (Figure 4). The Cd^{2+} atom was accommodated on the top of **1** and coordinated to both of the 2,2′-bipyridines. Host **1** underwent significant conformation adjustments from its unbound state to

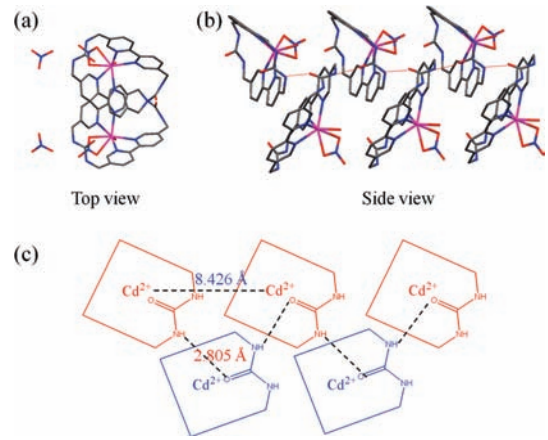

Figure 5. Extended structure of complex [Cd(host **1**)$(H_2O)(NO_3)_2$]. (a) Top view. (b) Side view showing the **1**·Cd^{2+} layer connected through 1D linear N(5)H(5)···O(2)═C hydrogen-bonding with ligands alternately slanted up and down in the layer. (c) A sketch of the layered structure illustrating the distance between the Cd^{2+} atoms.

yield an *endo*-type structure that affords a stable host **1**·Cd^{2+} complex. The 2,2′-bipyridines adopt a nearly planar conformation with N−C−C−N dihedral angles of 5.2°, and the four nitrogen donors point inward for efficient coordination with Cd^{2+}. The van der Waals distance between pyridine nitrogens of the recognition site decreased from 2.0 Å in the free macrocycle to 1.2 Å. As a consequence, the cadmium atom (radius ≈ 0.95 Å) is located slightly above the macrocyclic cavity, ∼1.77 Å above the mean plane of the macrocycle. The asymmetric unit of the crystal consists of one Cd(**1**)$(H_2O)^{2+}$ cation and two unique nitrate anions (one coordinated to the metal center and the other situated out of coordination sphere). Each Cd^{2+} atom is coordinated to four nitrogen atoms of bipyridines (Cd−N = 2.382(3)−2.436(3) Å) and to two oxygen atoms of the chelating nitrate group (Cd−O = 2.371(5)−2.557(4) Å) and an oxygen of water (Cd−O = 2.346(3) Å), respectively. The coordination environment of cadmium can be described as distorted octahedral. Indeed, it appears that host **1** can rotate and is able to access *endo*-type conformations as evidenced by this cadmium coordination complex.

Examination of the extended structure shows that urea carbonyl pointed in opposite directions as observed in other bis-urea macrocycles; however, the typical three-centered urea hydrogen bonds were not formed. As predicted by Hunter, the urea carbonyl forms one hydrogen bond to the NH on a neighboring macrocycle, but the basic nitrate counterion competes with the carbonyl for the other urea NH's, presumably because it is now more basic than an oxygen that is already involved in one hydrogen bond.[65] Thus, the individual host **1**·Cd^{2+} monomers are held together by a single chain of NH to urea carbonyl interactions with a distance of 2.805(4) Å from N(5)H(5)···O(2)═C and an angle of 175°. The **1**·Cd^{2+} complexes are arranged alternately slanting up and down in the layer, and the adjacent Cd···Cd distance within each row is kept at 8.43 Å (Figure 5). The remaining three urea N−H and one C═O on macrocycle formed hydrogen-bonding interactions with nitrate ions and water molecules (N(1)H(1)···O(6) 2.938(6) Å, N(2)H(2)···O(7) 2.918(7) Å, O(3)H(3A)···O(1) 2.838(4) Å, N(6)H(6)···O(8) 2.973(5) Å, O(3)H(3B)···O(9) 2.772(4) Å). We are currently investigating if columnar assembly could be

(64) Shannon, R. D. *Acta Crystallogr., Sect. A: Found. Crystallogr.* **1976**, *A32*, 751–767.

(65) Hunter, C. A. *Angew. Chem., Int. Ed.* **2004**, *43*, 5310–5324.

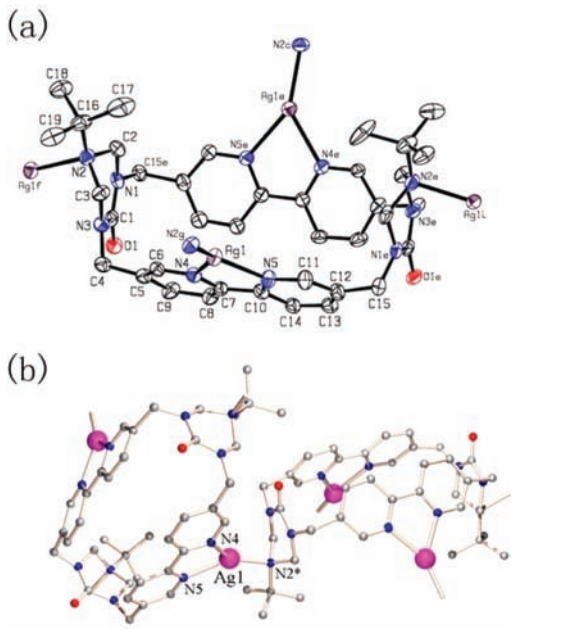

Figure 6. X-ray crystal structures of macrocycle **2**·Ag^+ complex {[Ag_2(host**2**)](SO_3CF_3)$_2$·unknown solvate}. (a) 30% probability displacement ellipsoid plot of the polymeric framework repeating unit, with atom labeling sequence. Hydrogen atoms omitted. (b) The coordination environment of the silver atom in **2**·Ag^+.

favored with metal salts that have less basic counterions, such as triflate, perchlorate, and acetate.

X-ray quality single crystals (colorless plate) of **2**·Ag^+ {[Ag_2(**2**)](SO_3CF_3)$_2$·unknown solvate} were obtained by solvent diffusion method (layering technique)[66] and revealed the metal coordinated in the *exo* coordination mode. Although the crystals were grown from a 1:1 ratio of host to metal salt, the crystalline complex displayed a 1:2 host:guest stoichiometry. Figure 6 gives a perspective view of the local coordination environment around the one crystallographically unique Ag(I) atom. The Ag(I) atom adopted a distorted trigonal planar configuration. The silver (Ag^+ radius ~1.0 Å for four-coordination, as three-coordination was not tabulated[64]) preferred an *exo*-coordination mode and was accommodated out of the macrocyclic cavity. Two sp^2 nitrogen atoms from one 2,2′-bipyridine chelate the Ag^+ in bidentate fashion, and there was an additional interaction between the Ag^+ and sp^3 nitrogen from *tert*-butyl-amine on a neighboring macrocycle in monodentate fashion (Figure 6b). The N−Ag−N angles range from 72.1° to 144.8°, and the Ag−N(*t*-Bu) distances range from 2.2 to 2.3 Å.

In the presence of silver, host **2** adopted an elliptic "bowl" shape with the 2,2′-bipyridines in a planar conformation to coordinate with silver atom, different from the conformation observed in the free host. The four nitrogen donors on 2,2′-bipyridine units point slightly outward with the urea carbonyls and the nitrogen donors also located in opposite directions to minimize dipole interactions. The *tert*-butyl units move from parallel in pure host to vertical, likely as a result of increased steric hindrance upon coordination. Although silver(I) usually favors linear two coordinate geometry with nitrogen donors, it can afford complexes with a number of different coordination

(66) A solution of $AgCF_3SO_3$ (4 mg, 0.015 mmol) in methanol (0.75 mL) was layered on top of a solution of **2** (10 mg, 0.015 mmol) in CH_2Cl_2 (0.75 mL). Colorless block-like crystals of Ag^+·**2** complex formed within two weeks.

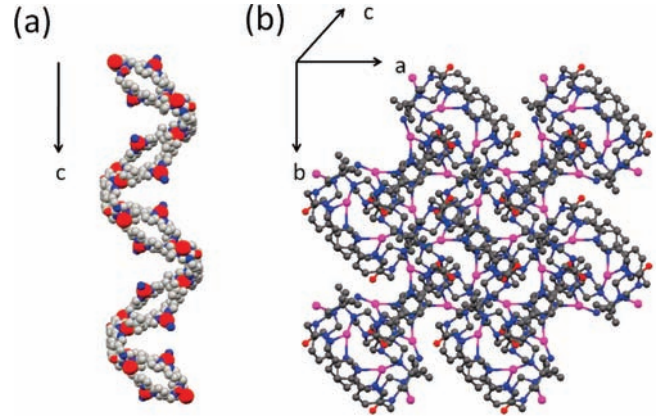

Figure 7. (a) Homochiral polymeric helix structure viewed perpendicular to the crystallographic *c* axis. (b) Infinite partially interlaced porous structure viewed parallel to the *c* axis.

geometries in the solid state.[67−69] It appears that silver(I) preferentially selected the *exo* conformation of host **2**, which supplies the 2,2′-bipyridine and a neighboring *tert*-butyl-amine as ligands.

The coordination of Ag^+ between two macrocycles leads to an infinite three-dimensional polymeric structure, crystallizing in the chiral tetragonal space group $P4_32_12$. The silver coordination induces an interplanar angle of 81.6° between two neighboring macrocycles, affording helical one-dimensional coordination polymers along the *c* axis with the pitch length of 32.6 Å as shown in Figure 7a. Typically, helical systems arising from achiral starting materials show an equal distribution of *P*- and *M*-helices, making them overall racemic. In this case, the helical coordination polymer was built by a 4_3 right-handed screw axis symmetry element and was homochiral. An interconnected network formed by the further assembly of these helices is shown in Figure 7b. Because each macrocycle molecule coordinates four silvers and forms two orthogonally arranged helices through the long *c* axis and short *a* axis, respectively, a view from the *c* axis shows an infinite partially interlaced porous structure with chiral channels. To date, only a few examples of helical coordination polymers with homochirality have been reported.[70−72] We are currently evaluating other host **2**·Ag^+ crystals to see if the other enantiomer crystallizes separately. Such chiral porous structures are rare and show potential in asymmetric catalysis, chiral sensing and separation.[73−75]

Complexation Behaviors of Host 1 in Solution. The solid-state structures of the free hosts and the two metal complexes suggested that both *endo* and *exo* metal coordination modes were accessible for these hosts. We next sought to evaluate whether

(67) *Comprehensive Coordination Chemistry*; Wilkinson, G., Ed.; Pergamon: Oxford, 1987; Vol. 5, p 786.
(68) Khlobystov, A. N.; Blake, A. J.; Champness, N. R.; Lemenovskii, D. A.; Majouga, A. G.; Zyk, N. V.; Schröder, M. *Coord. Chem. Rev.* **2001**, *222*, 155–192.
(69) Steel, P. J.; Fitchett, C. M. *Coord. Chem. Rev.* **2008**, *252*, 990–1006.
(70) Ezuhara, T.; K.; Aoyama, Y. *J. Am. Chem. Soc.* **1999**, *121*, 3279–3283.
(71) Xu, Y.; Han, L.; Lin, Z. Z.; Liu, C. P.; Yuan, D. Q.; Zhou, Y. F.; Hong, M. C. *Eur. J. Inorg. Chem.* **2004**, 4457–4462.
(72) Maggard, P. A.; Stern, C. L.; Poeppelmeier, K. R. *J. Am. Chem. Soc.* **2001**, *123*, 7742–7743.
(73) Tarducci, C.; Badyal, J. P. S.; Brewer, S. A.; Willis, C. *Chem. Commun.* **2005**, 406–408.
(74) Kitagawa, S.; Kitaura, R.; Noro, S. *Angew. Chem., Int. Ed.* **2004**, *43*, 2334–2375.
(75) Mueller, U.; Schubert, M.; Teich, F.; Puetter, H.; Schierle-Arndt, K.; Pastre, J. *J. Mat. Chem.* **2006**, *16*, 626–636.

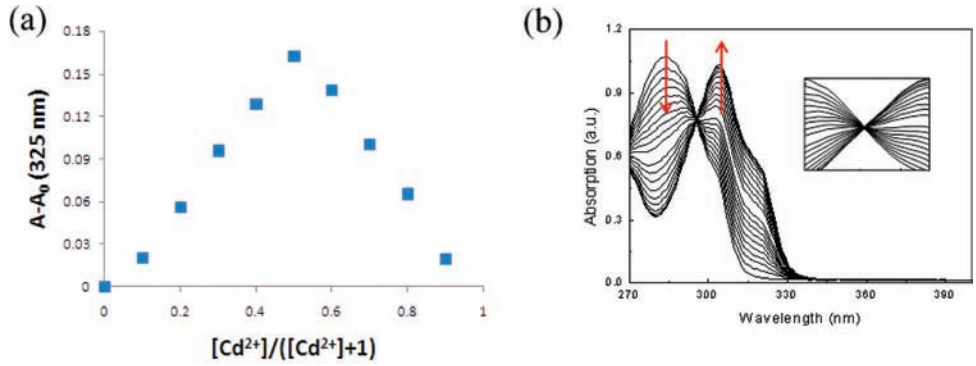

Figure 8. (a) JOB plot for host **1** and $Cd(NO_3)_2$ in THF and methanol mixed solvent (v/v = 99:1). The total concentration of **1** and metal salts was kept constant at 2.1×10^{-5} mol L^{-1}. The molar fraction of the metal salts varied in the range of 0.1−0.9, $\lambda_{obs} = 325$ nm.[76] (b) Titration curves of **2** solution (10^{-6} M) in THF at 298 K upon addition of aliquots of $Cd(NO_3)_2$.

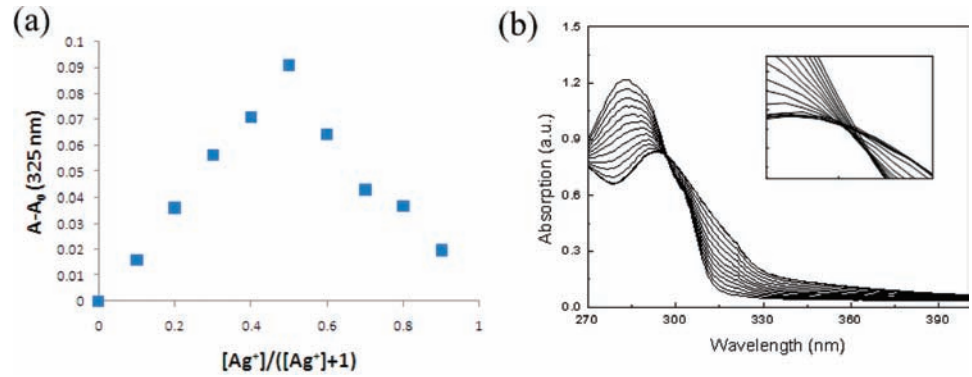

Figure 9. (a) JOB plot for host **1** and $AgNO_3$ in THF and methanol mixed solvent (v/v = 99:1). The total concentration of **1** and metal salts was kept constant at 2.1×10^{-5} mol L^{-1}. The molar fraction of the metal salts varied in the range of 0.1−0.9, $\lambda_{obs} = 325$ nm. (b) Titration curves of **2** solution (10^{-6} M) in THF at 298 K upon addition of aliquots of $AgNO_3$.

complexes with similar host:guest ratios can be formed in solution and to measure their association constants. Will specific metals show preference for one coordination mode over another? Or alternatively, will each metal form multiple complexes with both *exo* and *endo* coordination modes giving rise to several host:guest complexes? To investigate the metal ion binding properties of these macrocyclic ligands, we studied guest complexation by both host **1** and **2** using titration curves based on UV−vis spectroscopic analysis. UV−vis absorption spectra were recorded upon gradual addition of metal salts to the solution of macrocycle host. The titration curves obtained enabled the study of the binding process and provided a means to quantify complex stability. During the process, all nitrate salts were used to minimize the possible effects caused by counter-anions. Host:guest stoichiometry was determined through continuous variation plots (JOB plots).[76]

We first examined the interaction of host **1** with $Cd(NO_3)_2$ in solution as it was already known that this guest formed a 1:1 complex with the metal bound in an *endo* mode in the solid state. The UV−vis spectrum of free uncoordinated **1** (solvent THF/methanol (v/v = 99:1)) displayed absorption maxima at 283 nm with a shoulder at 300 nm. The wavelength and shape of the absorption band remained invariant over the concentration range of 2.1×10^{-6} to 2.1×10^{-5} mol L^{-1} in THF, suggesting that **1** did not aggregate in dilute solution (see Supporting Information). Upon addition of cadmium salts to the solution of **1**, the main absorption of free host **1** at 283 nm decreased, and at the same time, a new absorption generated at 304 nm, which can be assigned to charge transfer (CT) absorption of the forming metal complexes (Figure 8b). A clear isosbestic point at 296 nm was observed in the titration curves, indicating the formation of a single new complex. The absorbance at 325 nm was used to construct a JOB plot (Figure 8a). The JOB plot shows two lines that intersect at a mole ratio of 0.5, indicative of a 1:1 host:guest stoichiometry between host **1** and Cd^{2+}, which is consistent with the crystal structure. The steep intersecting lines suggested a high association constant. Given the JOB plot data and clear isosbestic point, we assume that during the titration process only three species exist: host, guest, and the host−guest complex. The binding constants between host **1** and Cd^{2+} was estimated with the nonlinear least-squares regression method to be very high, 1.5×10^8 M^{-1}.

We next examined the binding of silver ($AgNO_3$) by host **1**, which was expected to have a preference for *exo* coordination, as observed in the crystal structure with host **2**. The JOB plot also exhibited a 1:1 host:guest stoichiometry between host **1** and silver. Similar to the previous example, the addition of silver salts to the solution of **1**, the main absorption of free host **1** at 283 nm decreased as a new absorption generated at 293 nm (Figure 9b). In contrast to the host **1**·Cd complex, the titration with the silver does not display an ideal isosbestic point and showed a small drift. In addition the CT absorption of the new complex became very broad with concurrent increase baseline absorption at longer wavelength. The baseline absorption increase may reflect a visible phenomenon, and the mixture of host **1** and silver became turbid over time (within hours). We have not yet obtained crystals of this complex suitable for X-ray crystallography. In comparison, the absorption spectrum for

(76) Hirose, K. *J. Inclusion Phenom. Macrocyclic Chem.* **2001**, *39*, 193–209.

Table 2. Association Constants[81] between Host **1** and Metal Ions at 298 K

	Cd^{2+}	Zn^{2+}	Mn^{2+}
radius (Å)	0.97	0.74	0.46
K_a (M^{-1})	1.5×10^8	5.0×10^7	3.4×10^6

complex of **1** and cadmium showed a very smooth baseline, and the corresponding solution of the complex remained transparent over time. Our hypothesis is that these differences in spectral features may be associated with two distinct coordination modes: an *endo* coordination for cadmium, as observed in the crystal structure, versus an *exo* coordination for the silver, which could potentially further assemble to yield oligomers and polymers. Such an assembly process could include a number of different association constants.

To further investigate the issue of size, we next screened a series of metal salts with ionic radii between 0.46 and 0.74 Å (Mn^{2+}, Fe^{3+}, Co^{2+}, Ni^{2+}, Cu^{2+}, and Zn^{2+}) with the expectation that some of these metals might favor *endo* coordination as observed in the solid state for Cd^{2+}. Each metal was screened with host **1** using UV titrations and JOB plots. With the exception of Fe^{3+}, all of the metals tested clearly displayed the formation of 1:1 host:guest complexes by JOB plot studies (Supporting Information). In contrast, for Fe^{3+} the JOB plot showed no maximum, and its host:guest stoichiometry could not be determined, suggesting that Fe^{3+} might form multiple weak complexes. All other metals showed titration curves where the main absorption of free host **1** at 283 nm decreased as a new absorption was generated at longer wavelengths, suggesting the formation of metal complexes. However, only two metals, Mn^{2+} and Zn^{2+}, displayed a single isosbestic point and a smooth baseline, similar to what was observed in the case of cadmium. Our hypothesis is that these three metals (Cd^{2+}, Mn^{2+}, and Zn^{2+} ($r \approx 0.74-0.95$ Å)) form discrete host:guest complexes with only three species (host, guest, and the host−guest complex) in solution. A second set of metals (Ag^+, Co^{2+}, Ni^{2+}, Cu^{2+} ($r \approx 0.69-1.0$ Å)) displayed no fixed isosbestic point and showed an increase in the baseline absorption at longer wavelengths, suggesting multiple intermediates are generated before a final 1:1 complex is formed. Clearly these metals span a range of sizes and no simple correlation was observed.

The binding constants between host **1** and the metal ions that show 1:1 stoichiometry with clear isosbestic points (Cd^{2+}, Zn^{2+}, and Mn^{2+}) were determined with the nonlinear least-squares regression method.[76] Values of the association constants (K_a) were determined using standard UV titration methods at concentrations around 10^{-6} M and are summarized in Table 2. Host **1** shows higher affinity for Cd^{2+} ($K_a = 1.5 \times 10^8$ M^{-1}) versus Zn^{2+} or Mn^{2+} ($Cd^{2+} > Zn^{2+} > Mn^{2+}$). This is quite different from the Irvings−Williams order, which refers to the relative stabilities of complexes formed by a metal ion in water. Simple bipyridines and linear oligobipyridines adhere to the Irving−Williams series in many solvents.[77−80] The deviation from this order experimentally suggests something unusual is occurring, perhaps selection of the cation to match the cavity formed from the host's *endo* conformation based on size and

Scheme 3. Sketch of the Two Types of Coordination Modes of Host **1**

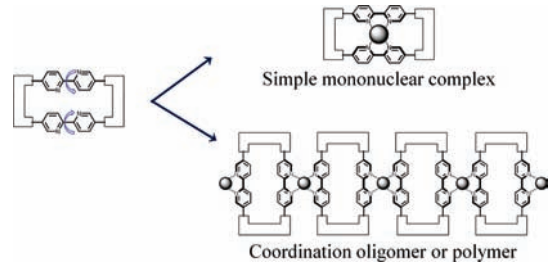

coordination geometry. Indeed, both the high binding constant observed for Cd^{2+} in solution and the coordination complex observed in the solid state, indicated that Cd^{2+} was well matched in size, shape, and coordination geometry for the *endo* conformer of host **1**. In addition, the observed 1:1 binding stoichiometry in solution and the clear isosbestic point lead us to propose that the complex host **1**·Cd^{2+} in the solution state was similar in structure to the *endo*-coordination complex observed in the solid state. We surmise that the host **1**·Zn^{2+} and the host **1**·Mn^{2+} are also *endo*-coordination complexes. These three metals may be more flexible in choosing coordination geometries and coordination numbers due to their full or half occupied *d* atomic orbitals and may be able to better coordinate to the four pyridines of host **1**, which are constrained by the macrocycle.

The slight drift of the isosbestic point for the second series of metals (Ag^+, Co^{2+}, Ni^{2+}, and Cu^{2+}) suggested that there may be several steps or intermediates in the host−guest complexation process. Our hypothesis is that these metals form *exo*-coordination complexes. The binding of a metal to an *exo*-oriented bipyridine would leave open sites for further coordination with an *exo*-oriented bipyridine from a second macrocycle. Such complexes may further assemble into oligomers (Scheme 3), although overall they would still display 1:1 host:guest stoichiometry, which we observed in the JOB plots. The separate, stepwise coordination of the metal center may not give a clear isosbestic point as several intermediates are formed.[82] The growth of the oligomer over time could lead to polymers with lower solubility.

In the titrations of host **1** with this second set of metal nitrate salts (Ag^+, Co^{2+}, Ni^{2+}, and Cu^{2+}), we observed an increase in the baseline absorbance at longer wavelengths (Figure 8b and Supporting Information). Such an increase could result from poor solubility of the metal complex, from the intrinsic absorption of the metal complexes, or from Rayleigh scattering induced by long coordination oligomers or polymers. We probed the origin of this baseline absorption by a light transmittance study using a UV−vis spectrophotometer at a fixed wavelength of 800 nm and by Gel Permeation Chromatography (GPC). Common organic compounds generally show no absorption at 800 nm,[83] which was true for free host **1** and the host **1** complexes with Cd^{2+}, Zn^{2+}, and Mn^{2+}. The transmittance

(77) Gong, H. Y.; Wang, D. X.; Zheng, Q. Y.; Wang, M. X. *Tetrahedron* **2009**, *65*, 87–92.
(78) Abe, Y.; Wada, G. *Bull. Chem. Soc. Jpn.* **1981**, *54*, 3334–3339.
(79) Kaim, W. *J. Am. Chem. Soc.* **1982**, *104*, 3833–3837.
(80) Tori, Y.; Yazaki, T.; Kaizu, Y.; Murasato, S.; Kobayashi, H. *Bull. Chem. Soc. Jpn.* **1969**, *42*, 2264–2267.

(81) Titrations were performed by adding small aliquots (3−5 μL) of guest solution (10^{-4} mol L^{-1}) in THF and MeOH mixed solution (v/v = 99:1) into 2 mL of host solution (10^{-6} mol L^{-1}) in THF and MeOH mixed solution (v/v = 99:1) by using a microsyringe. UV−vis absorption changes were monitored during the titration. The difference in absorbance (ΔA) of the host in the presence of the guest and absence of the guest was recorded, and the data were plotted against [guest].

(82) Giansante, C.; Ceroni, P.; Venturi, M.; Balzani, V.; Sakamoto, J.; Schluter, A. D. *Chem.—Eur. J.* **2008**, *14*, 10772–10781.
(83) Ravi, P.; Dai, S.; Tam, K. C. *J. Phys. Chem. B* **2005**, *109*, 22791–22798.

Table 3. Transmittance Changes at 800 nm over Time for Host **1**·Metal Complexes

	light transmittance (%)			
complex	0 min	10 min	30 min	60 min
1· Cd^{2+}	99.8	99.8	99.8	99.8
1· Ag^{+}	100.1	98.0	86.4	84.3
1· Cu^{2+}	100.1	99.4	96.6	81.0
1· Ni^{2+}	100.0	99.8	97.3	81.2

changes at 800 nm of the equivalent mixtures between **1** and metals in THF solution (10^{-4} M) were monitored. Table 3 shows the transmittance changes at 800 nm of the mixtures between **1** and metals in THF solution. Although the host **1**·Cd^{2+} complex did not show any change in light transmittance over time, the silver, copper and nickel complexes all showed a decrease in transmittance at 800 nm and over time become visibly turbid.

GPC was further conducted on the freshly prepared host **1**·Cu^{2+} complex in THF (1:1 molar ratio), which showed clear scattering at 800 nm. Although most of the complex remained on the membrane filter, a chromatogram of the filtrate displayed a broad peak with an average molecular weight of ca. M_n = 26300 (M_w/M_n = 1.622) (see Supporting Information). Under the same conditions no peak was observed in this high-molecular-weight region for pure **1**. These preliminary studies suggest that tetradentate host **1** may be forming some oligomeric complexes with Ag^{+}, Co^{2+}, Ni^{2+}, and Cu^{2+}. We will report more on these in due course.

Next we examined the ability of hexadentate host **2** to form coordination complexes in solution. In the solid state, this host formed a 1:2 host **2**·Ag^{+} complex with the silver and was coordinated in a bidentate fashion between a 2,2′-bipyridine from one macrocycle to an sp^3 nitrogen of the triazinanone on a second macrocycle. We were curious to see if host **2** would form discrete 1:2 host:guest complexes in solution or if polymeric coordination complexes would be observed. The UV−vis spectrum of free uncoordinated **2** displayed absorption maxima at 285 nm with a shoulder at 305 nm. Upon addition of silver salts to the solution of **2**, spectral changes similar to those of host **1** were observed: the main absorption of free host **2** at 285 nm decreased and concurrently a new CT absorption of complex was generated at longer wavelengths (295 nm). The JOB plot analysis in solution revealed a 1:2 host:guest stoichiometry between host **2** and silver nitrate (Figure 10a). The UV titration for the host **2**·Ag^{+} complex displayed a clear isosbestic point, smooth baseline absorption, and a narrow peak-width of CT absorption band. These observations suggest that in contrast to the polymer assembly observed in the solid state, a discrete 1:2 host **2**·Ag^{+} complex was rapidly formed in solution.

Given the structure of the 1:2 host **2**·Ag^{+} complex observed in the solid state, it is likely that the triazinanone amine acts as additional donor site to enhance the coordination potential of the single 2,2′-bipyridine. Therefore, we propose a binuclear coordination structure for host **2**·Ag^{+} complex in solution at these low concentrations (10^{-5} M) where two metal ions are coordinated above and below the macrocyclic plane of **2** with the central silver coordinated to the bipyridine and the triazinanone tertiary amine (Scheme 4).

We further studied the complexation properties of host **2** in solution with a series of other transition metal ions (Cd^{2+}, Zn^{2+}, Cu^{2+}, Ni^{2+}, Co^{2+}, Fe^{3+}, Mn^{2+}, and Cr^{3+}). Some metals (Fe^{3+}, Mn^{2+} and Cr^{3+}) displayed very weak interactions with host **2** and the host:guest stoichiometry could not be determined by JOB plots. Host **2** showed high affinity for other metals, including Cd^{2+}, Zn^{2+}, Cu^{2+}, Ni^{2+}, and Co^{2+}. JOB plots for host **2** and this series of metals are consistent with the metals forming host:guest complexes with 1:2 stoichiometries. In addition, each of the respective UV titration curves displayed clear isosbestic points and smooth baseline absorptions (see Supporting Information).

The binding constants for the 1:2 host **2**·metal complexes were estimated with nonlinear least-squares regression methods with two binding constants that represent the two coordination steps (Table 4). On first observations, one notes that the K_1

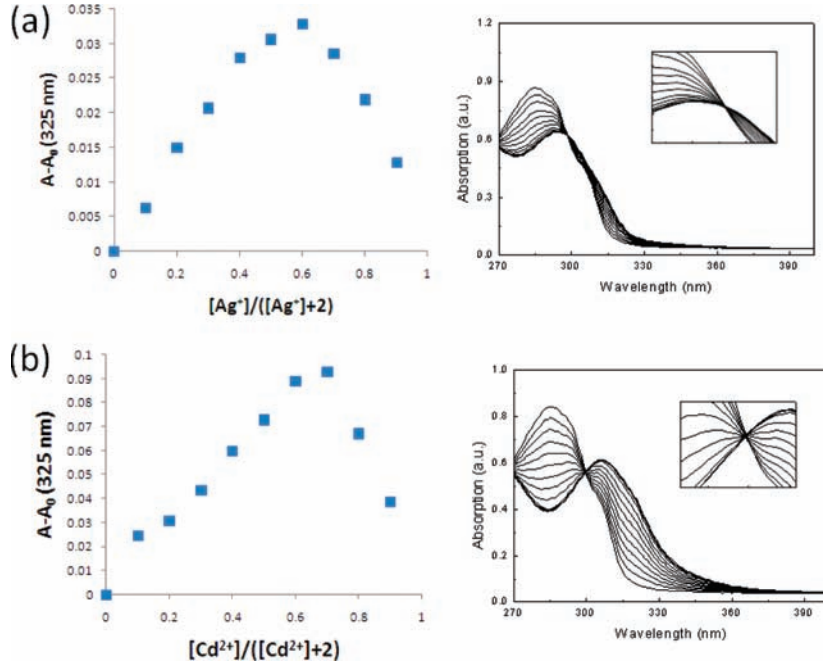

Figure 10. JOB plot for host **2** and (a) $AgNO_3$, (b) $Cd(NO_3)_2$ in THF and methanol mixed solvent (v/v = 99:1). The total concentration of **2** and metal salts was kept constant at 1.5×10^{-5} mol L^{-1}. The molar fraction of the metal salts varied in the range of 0.1−0.9, λ_{obs} = 325 nm. Titration curves of **2** solution (10^{-6} M) in THF at 298 K upon addition of aliquots of (a) $AgNO_3$ and (b) $Cd(NO_3)_2$.

Table 4. Binding Constants between Host **2** and Metal Ions at 298 K

	Ag^+	Cd^{2+}	Zn^{2+}	Cu^{2+}	Ni^{2+}	Co^{2+}
K_1 (M^{-1})	1.6×10^6	8.1×10^6	1.9×10^6	1.7×10^8	4.6×10^7	1.4×10^8
K_2 (M^{-1})	1.4×10^5	6.9×10^2	very small	3.3×10^5	4.3×10^3	4.1×10^4

Scheme 4. Schematic Representation of Complex of Host **2** with Silver

values were large and range from a high of 1.7×10^8 (for Cu^{2+}) to 1.6×10^6 (for Ag^+). Host **2** binding affinities followed the order of $Cu^{2+} > Co^{2+} > Ni^{2+} > Fe^{3+}$ and Mn^{2+}, as predicted by the Irving−Williams order.[77] In contrast to host **1**, it appears that host **2**, shows no unusual size effects in the complexation process. The binding constants are similar to what is observed for simple 2,2′-bipyridines.[78−80] We propose that host **2** binds this series of metals via a single conformation, an *exo* conformer, which would be expected to give 1:2 binding stoichiometry in contrast to the *endo* conformer. The K_2 values were found to be much smaller than K_1, the expected result of electrostatic repulsion between two metal centers. The lower K_2 values were consistent with stable 1:2 host:guest complexes, which generally had lower propensities to form oligomers.

In summary, we have synthesized two new macrocyclic ligands containing conformationally mobile 2,2′-bipyridine groups bridged by either ureas or triazinanone units. The flexible connections appeared to allow the metal binding sites to freely rotate and thus favor the structures that best accommodate the guest. The solid-state structures demonstrated that the bipyridine units adopted similar conformations in both free hosts, in which the bipyridines did not adopt either *endo* or *exo* orientations. Complexation of Cd^{2+} by host **1** resulted in a switch in the bipyridine conformation to favor an *endo* structure, in which the four bipyridine nitrogens were pointed inward coordinating to a single cadmium atom. This host **1**·Cd^{2+} complex [Cd(**1**)$(H_2O)(NO_3)_2$] formed layered structures with regular 8.426 Å Cd···Cd spacing enforced by one-dimensional NH···O═C hydrogen bonding. Complexation of silver ion by host **2** also caused a conformational change in the host and the bipyridine ligands twisted outward to afford an *exo*-coordination site for the host **2**·Ag^+ structure ([Ag_2(**2**)]$(SO_3CF_3)_2$·unknown solvate). These solid-state structures demonstrated that the metal binding site was able to access multiple conformations. We are beginning to explore large metals (Eu, Er, and Ru) whose size should have a preference for *exo*-coordination modes. Such complexes may have interesting optical properties.

In solution, the two hosts displayed different types of complexation behavior. Host **1** consistently formed complexes with 1:1 host:guest stoichiometry and showed relative metal complex stabilities that differed from the Irving−Williams order, suggesting that something unusual was occurring that differed from typical bipyridines. Complexes of tetradentate host **1** with Cd^{2+}, Zn^{2+}, and Mn^{2+} showed high binding constants, and we predict that in solution these complexes have the metal bound within the macrocyclic cavity. A second series of metal nitrate salts also showed 1:1 binding with host **1** but UV titration curves showed no clear isosbestic point and significant increases were observed in the baseline at longer wavelengths. Our hypothesis is that these metals form *exo*-coordination complexes that may further associate into oligomers. We are currently studying this series and are trying to establish their structure by solid-state methods.

In contrast, the hexadentate host **2** displayed more uniform interactions with the series of metal nitrate salts tested. All the metals tested showed 1:2 host:guest stoichiometry and clear isosbestic points in their UV titrations. The metal complex stabilities followed the expected Irving−Williams order as indicated by their K_a's. The different complexation behaviors of host **2** is likely due to the presence of additional basic tertiary amines that enhance the coordination potential of single 2,2′-bipyridine and likely stabilizes *exo* complexation of these metals.

The reported hosts combined bipyridine metal binding sites with a second functional group (ureas in host **1** and tertiary amines in host **2**). The additional functionality has the potential to guide further assembly of the metal complexes into coordination polymers, as observed in the helical structure of the host **2**·Ag^+ complex. Alternatively, these pendent functional groups open up new possibilities for anion binding and catalysis. We are currently focused on assessing these new hosts as building blocks for 3D supramolecular self-assembly and will report on this in due course.

Acknowledgment. The authors gratefully acknowledge support in part for this work from the NSF (CHE-071817), from the Petroleum Research Fund (44682), and from a grant from the University of South Carolina, Office of Research and Health Sciences. Synchrotron data were collected through the SCrALS (Service Crystallography at Advanced Light Source) program at Beamline 11.3.1 at the Advanced Light Source (ALS), Lawrence Berkeley National Laboratory. The ALS is supported by the U.S. Department of Energy, Office of Energy Sciences Materials Sciences Division, under contract DE-AC02-05CH11231.

Supporting Information Available: ^1H, ^{13}C, and variable temperature ^1H NMR spectra of hosts; X-ray crystallographic files in CIF format for **1**, **2**, [Cd(**1**)$(H_2O)(NO_3)_2$], and [Ag_2(**2**)]$(SO_3CF_3)_2$. This material is available free of charge via the Internet at http://pubs.acs.org.

JA906474Z